Nonlinear surface impedance $Z(T,f,H_{rf})$ of Tl-Ba-Ca-Cu-O thin films

E. Gaganidze, R. Heidinger, J. Halbritter, A. Shevchun, M. Trunin, and H. Schneidewind

***Abstract*—$YBa_2Cu_3O_7$ (YBCO) film quality has reached a stage enabling rf applications at $T \leq 80$ K. Higher operating temperatures or better power handling are very much desired. $Tl_2Ba_2CaCu_2O_8$ (Tl-2212) is a perfect candidate with its higher transition temperature $T_c > 100$ K. We studied the rf field dependence of the impedance Z_s of epitaxial Tl-2212, which shows already surface resistances at low fields superior to YBCO and promising power handling with a nonlinearity onset above $\mu_0 H^* \simeq 3$ mT. Defective Tl-2212 films show anomalous non-linear behavior for $\mu_0 H_{rf} \leq \mu_0 H^* \sim 0.3$ to 1 mT, extremely pronounced at $T < 40$ K, indicating the presence of very weak-links yielding flux-flow, followed at higher fields $\mu_0 H_{rf} \gtrsim 0.5$ mT by hysteresis losses with a linear field dependence $\delta R_s(H_{rf}) \propto H_{rf}$. Better quality Tl-2212 films show $\delta R_s(H_{rf}) \propto H_{rf}^2$ up to fields of about 5 to 10 mT. The $\delta R_s(H_{rf}) \propto H_{rf}^{\,n}$ (n=1,2) dependencies together with the ratios $r(T) = \delta X_s / \delta R_s \sim 1$ to 10 hint to hysteresis losses of Josephson fluxons enhanced by slits or holes in the films.**

Index Terms— superconducting films, surface impedance, nonlinearity

I. INTRODUCTION

HIGH-TEMPERATURE superconducting (HTS) thin films find already wide application in passive microwave devices [1], as e.g. miniaturized thin film filters. Thin films of 2nd generation, such as Tl-2212, allow new applications, because of their higher T_c and lower $R_s(T \leq 77\text{K})$ compared to YBCO. The rf field dependence of the surface impedance $Z_s = R_s + iX_s$ remains as a main obstacle. In spite of intensive research since several years, the mechanisms, material science, and rf fields causing non-linear behavior of Z_s of HTS films are not fully understood [2]-[9]. Whereas YBCO films have reached consistently high rf field levels, Tl-2212 have not reached this quality, yet. Hence, the identification and quantification of defects on a 100 µm-scale (dielectric segregates, holes, cracks) and on a nm-scale (weak- or strong-links) are essential. The 100 µm scale defects are detrimental due to nonlinearities caused by field enhancement inducing fluxoids. On the nm-scale non-linear mechanisms of Z_s include e.g. pair-breaking in the BCS Meissner state [2],[3], creation, pinning and flow of Abrikosov vortices [4],[5], leakage current losses in the weak link Meissner state [2],[6] or creation, pinning [2],[7],[8] and flow [2],[5],[9] of Josephson fluxons. The complexity of the Tl-2212 growth process and of the resulting morphology, the electronic, and the chemical structure of the material and their relation to $Z_s(H_{rf})$ show the need of careful analysis of various defects and nonlinearities and their temperature- and frequency-dependencies, which is the aim of the present work.

II. EXPERIMENTAL

Tl-2212 films have been manufactured on CeO_2-buffered sapphire by annealing a $Ba_2CaCu_2O_x$ precursor at 860° in a $Tl_2O + O_2$ atmosphere [10] through a solid-state reaction. Some properties of the films for these investigations are listed in Table I. The island size of Tl-2212 on CeO_2/Al_2O_3 is with $a_J \simeq 1$ to 3 µm still larger than for YBCO with $a_J \leq 0.4$ µm. The rf field dependence of $Z_s = R_s(H_{rf}) + iX_s(H_{rf})$ was studied using a two port TE_{011} dielectric resonator techniques at 8.5 GHz (described in [8]) and 15.3 GHz using a sapphire puck with $\varnothing = 8$ mm and h = 4.8 mm. Unloaded quality factors Q_0 were measured for a weakly coupled resonator in the frequency domain by fitting the transmitted rf power with a Lorentz function. For high rf power, the input port of the resonator was strongly coupled. In order to avoid heating of the films, at moderate and high rf powers the loaded quality factor Q_L was determined in the time domain through analysis of the decay time after short microwave pulses ($\Delta t = 200$ µs to 1 ms) [11]. The relative change of the surface reactance was calculated from the measured resonance frequency change according to $\delta X_s = -2\Gamma_{\text{film}}\, \delta f/f$ (Γ_{film} is the geometry factor of the film in the R_s calculation).

TABLE I
PARAMETERS OF INVESTIGATED TL-2212 FILM

film	∅ [inch]	t [nm]	T_c [K]	j_c(77K) [MA/cm²]
C007-3b	2	400	103	2.5 to 3.5
C136-2b	3	< 400	100	1.0 to 2.0
C138-2a(A)	3	370	100	1.7 to 2.0
C138-2a(B)	3	370	103	2.0 to 2.4

Manuscript received August 6, 2002. This work was performed as part of German BMBF project “Supraleiter und neuartige Keramiken für die Kommunikationstechnik der Zukunft”.

E. Gaganidze, R. Heidinger, and J. Halbritter are with the Forschungszentrum Karlsruhe, IMF I, P.O. Box 3640, D-76021 Karlsruhe, Germany (+49-7247- 825921, Fax. +49-7247-824567, e-mail: ermile.gaganidze@imf.fzk.de).

A. Shevchun and M. Trunin are with Institute of Solid State Physics RAS, 142432 Chernogolovka, Moscow district, Russia.

H. Schneidewind is with the Institute for Physical High Technology (IPHT) Jena, D-07702 Jena, Germany (+49-3641-206114; fax: +49-3641-206199; e-mail: schneidewind@ipht-jena.de).

TABLE II
FIT PARAMETERS OF INVESTIGATED TL-2212 FILM

film	T [K]	f [GHz]	A [mΩ]	B (H_{rf} > 1 mT) [mΩ/10mT]	C (H_{rf} > 1 mT) [mΩ/(10mT)^2]	η [mΩ]	H_0 [mT]	H^* [mT]	$r = \delta X_s/\delta R_s$
C007-3b	6	8.5	-0.6	2.6	–	2.3	0.2	0.1	0.5
C007-3b	20	8.5	-0.36	2.8	–	2.0	0.17	< 0.1	0.4
C007-3b	30	8.5	-0.35	3.2	–	1.92	0.1	< 0.1	–
C007-3b	40	8.5	-0.18	3.1	–	1.75	0.1	< 0.1	–
C007-3b	77	8.5	1.16	4.6	–	0.66	0.09	< 0.1	–
C138-2a (A)	10	8.5	-0.09	1.72	–	< 0.1	–	1	1.0
C138-2a (A)	20	8.5	-0.10	2.00	–	< 0.1	–	1	1.1
C138-2a (A)	30	8.5	-0.02	1.76	–	< 0.1	–	1	1.0
C138-2a (A)	40	8.5	-0.05	2.09	–	< 0.2	–	1	1.1
C138-2a (A)	77	8.5	0.22	2.36	–	< 0.1	–	1	–
C138-2a (B)	77	8.5	0.25	0.09	0.60	–	–	3.0	–
C136-2b	20	8.5	0.15	–	0.39	–	–	3.1	8.5
C136-2b	55	8.5	0.29	–	1.0	–	–	2.7	6
C136-2b	77	8.5	0.51	–	3.1	–	–	2.1	4.4
C136-2b	10	15.3	0.7	–	0.7	–	–	4.9	9.2
C136-2b	20	15.3	0.88	0.2	0.46	–	–	5.7	9.0
C136-2b	40	15.3	1.26	0.36	0.8	–	–	4.6	6.6
C136-2b	60	15.3	1.46	–	3.3	–	–	3.8	5.0
C136-2b	77	15.3	2.05	–	4.0	–	–	1.75	3.9

III. EXPERIMENTAL RESULTS

SEM images of Tl-2212 film on CeO_2/Al_2O_3 show island sizes of about 1 to 3 µm. Smaller Tl-Ca-Cu-O and larger BaO segregates as well as µm-size holes are often visible on the terrace like film structure. Optical transmission images sometimes revealed circular spots of diameter $\varnothing \geq 100$ µm and density of 0.3 hole/cm^2, which are likely holes, related to corrosion by local elements [12]. Holes or segregates neither enhance the average Z_s at low rf fields in TE_{011} modes nor show up in j_c-maps and thus prove their insulating nature. These defects are related to the complex phase diagrams of the Tl-2212. Fig.1 shows a two dimensional R_s(145GHz)-map of sample C138-2a showing defects on a mm scale measured by R_s > 125 mΩ (A). As inferred from Table I, the j_c of the defective area is reduced only by 15% from its mean value, indicating that the observed defects are not resolved by low frequency transport properties. The latter result is supported by laterally resolved T_c measurement. Here *dc* conductivity measurement in the defective area revealed a reduction of T_c by $\Delta T_c \sim 2$ to 3 K only, but no percolation analysis was performed to define weak link properties [2]. The average temperature dependence $R_s(T, 8.5\text{ GHz})$ of C138-2a is shown in Fig.2, indicating the dominance of R_{res} in Tl-2212 films below 80 K for $f \lesssim 10$ GHz.

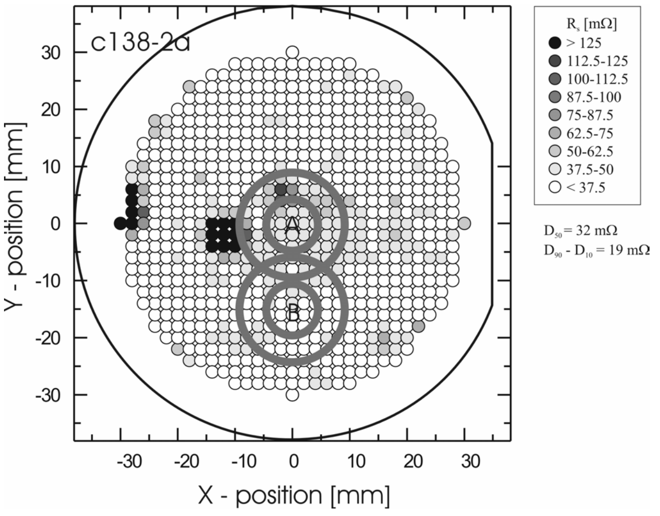

Fig. 1. R_s(145 GHz)-map of C138-2a. Positions (A) and (B) are

Table II, Fig.2 and 3 show the effective surface resistance R_s versus H_{rf} of different Tl-2212 films being not corrected for the finite film thickness (~ 400 nm). The $R_s(T,H_{rf})$-dependence was parameterized by the following equation

$$R_s(T,H_{rf}) = A(T) + B(T)\mu_0 H_{rf} + C(T)(\mu_0 H_{rf})^2 + \eta(T)(H_{rf}/(H_{rf}+H_0))^{1/2} \quad . \qquad (1)$$

including linear *hysteresis* losses [2], a quadratic term for losses due leakage losses through *weak links* [2], and a square

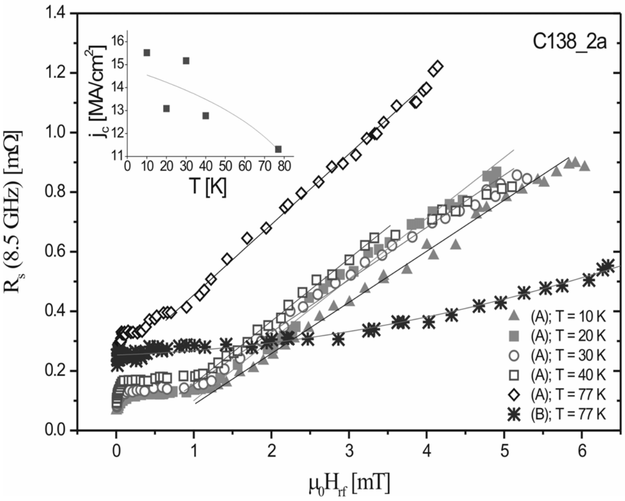

Fig. 2. R_s on H_{rf} for sample C138-2a with j_c (T) as inset.

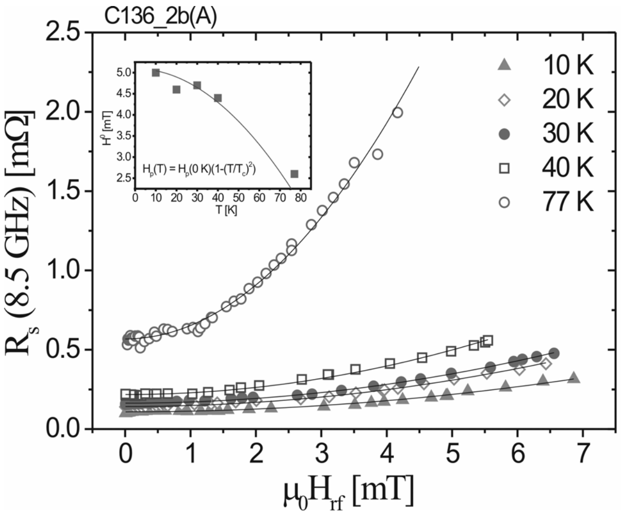

Fig. 3. R_s on H_{rf} for sample C136-2b(A) with $H^0(T)$ as inset.

root term for *flux-flow* losses [5]. Best Tl-2212 films, like C138-2a(B) in Fig.1, show good power handling with low field R_s(77K,8.5GHz) ≈ 0.25 mΩ, C < 1 mΩ/(10mT)^2 and 'turn-up' fields above $H^* \geq 3$ mT, see Table II and [9]. Most Tl-2212 films show $R_s(H_{rf})$-increases with A ~ 0.35 to 1.16 mΩ and C ~ 1.6 to 3.9 mΩ/(10mT)^2 that qualitatively resembles those of *mid* and *low* quality YBCO films [8]. Here $C(T)$ increases with T (Fig.3). C007-3b reveals an additional anomalous *non-linear* term at low rf fields being in contrast to conventional *TE*-mode $R_s(H_{rf})$-nonlinearities [8]. A *convex* $R_s(H_{rf})$-curvature is observed growing into linear $R_s(H_{rf}) \propto H_{rf}$ increases for H_{rf} > 0.3 mT. The depth of the *convex* curvature is enhanced towards lower temperatures accounted for by $\eta(T)$ listed in Table II together with H^* and $r = \delta X_s/\delta R_s$, discussed below. Similar to C007-3b, C138-2a(A) shows at H_{rf} < 0.3 mT a *convex* $R_s(H_{rf})$-curvature which is hardly resolved on this scale (Fig.2). Above H_{rf} > 1 mT C138-2a(A) shows strong linear $R_s(H_{rf})$-dependencies (Fig.1 and 2), whereas at position (B) a typical small quadratic $R_s(H_{rf})$-increase is found only [8]. The strong linear $R_s(H_{rf}) \propto H_{rf}$ -increase with $r(T) \approx 1$ observed at position (A) (Fig.2) closely correlates with the R_s(145GHz)-map in Fig.1, where a defective area is identified at a radial distance of 8 to 16 mm, which is partially probed by the TE_{011}(8.5GHz) mode. Such localized defective areas identified by R_s(145GHz) ≥ 120 mΩ yield large R_s-values and strong $R_s(H_{rf})$ nonlinearities at ~ 10 GHz (Fig.2) as proven already [8]. C136-2b (Fig.3) shows at both, 8.5 and 15.3 GHz, an enhanced $R_s(H_{rf}) \propto H_{rf}^2$ increase extremely pronounced at 77 K. There the 8.5 GHz data are scaled with a prefactor of $(15.3/8.5)^2$ giving a direct insight into the frequency dependencies.

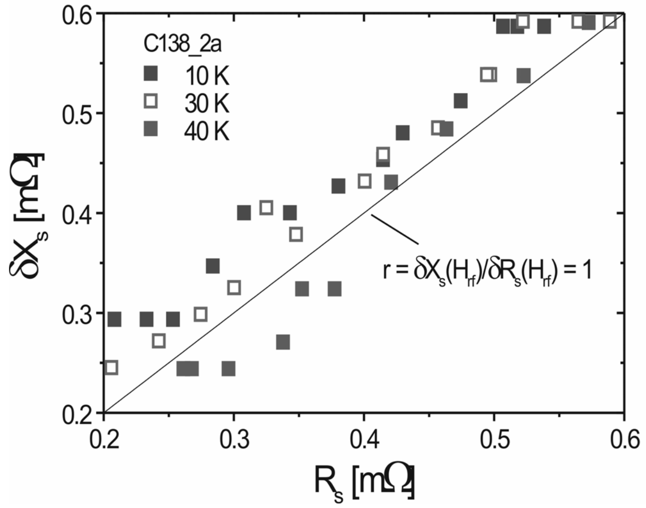

Fig. 4. Change of δX_s in dependence on R_s for sample C138-2a.

Fig.4 shows the relative change of the effective surface reactance δX_s with rf field H_{rf} versus corresponding effective surface resistance $R_s(H_{rf})$ for C138-2a. The temperature independent slope $r = \delta X_s/\delta R_s$ was found with r ~ 1. Results on r – values at 8.5 and 15.3 GHz are summarized in Table II decreasing from 9 at 20 K to r ~ 4 at 77 K (for C1136-2b).

IV. DISCUSSION AND SUMMARY

The temperature dependencies of R_s of Tl-2212 in Fig.2 below 0.5 $T_c \simeq$ 50 K and at $f \lesssim$ 10 GHz can be fitted with

$$\begin{aligned} R_{res}(T,\omega) &\cong 2\left[\omega\mu_0\lambda_{\text{int}}(T)\right]^2 \lambda_J^3(T)\Big/ a_J R_{bl} \\ &\propto \omega^2\Big/ j_{cJ}(T) a_J \left(j_{cJ}(T) R_{bl}^2\right)^{1/2} \end{aligned} \tag{2}$$

from [2] using λ(77K) ≈ 320 nm [13], a_J ≈ 1 µm, and R_{bl} ≈0.1 nΩcm^2 yielding the Josephson critical current density j_{cJ}(77K) ≈ 1 MA/cm^2, a value comparable to j_c listed in Table I (λ_J: Josephson penetration depth). Weak-links yield large R_{res}(T) contribution to R_s at 77 K, in contrast to YBCO with its shoulder at 40 to 60 K indicative for an intrinsic strong $\lambda(T)$-decrease [2]. The frequency dependence of $R_{res}(H_{rf} \ll H_{c1J})$ for C136-2b in Table II follows ω^β scaling with β ~ 2.4 το 3.0, stronger than ω^2–dependence of R_{res} and of R_{int}. Intrinsic $R_s(H_{rf})$-nonlinearities for Tl-2212 compounds are expected to occur at $H_{rf} > H_{c1}$(77K) ~ 10 mT [13],[14], *i.e.* at fields where Abrikosov fluxons enter into HTS film. The nonlinearities found in this work occur at much lower fields ~ 0.1 to 1 mT proving their extrinsic nature. The $\delta R_s(H_{rf}) \propto H_{rf}^n \propto \delta X_s(H_{rf})$ increase with n ~ 0.5 to 2 and r-values of 1 to 10 (Table II) hints to losses by Josephson fluxons [2],[8]. $R_s(T \leq 0.8T_c) \simeq R_{res}(T)$ is supported by the close relation between $R_s(\leq 0.8T_c) \approx R_{res}$ and nonlinearities in Tl-2212-films [9].

As found for *mid* quality YBCO films, C138-2a shows at 77 K low R_s(8.5GHz) ~ 0.25 mΩ and good power handling with C = 0.65 mΩ/(10mT)^2 at position (B). In contrast, C007-3b shows qualitatively new features in the $R_s(H_{rf})$-dependence at H^* < 0.1 mT [9], not found in our YBCO-films. Indeed, C007-3b shows a *convex* curvature at low rf fields followed by a linear $R_s(H_{rf})$-increase above 1 mT. Here the last term of Eq.(1) accounts for the Josephson *flux-flow* losses in *weak* weak-links, characterized by reduced j_{cJ} and $H_{c1J} \ll$ 1 mT. The *flux-flow* scaling field H_0 is reduced on increasing temperature for T < 30 K [9] as predicted for SNS junction, whereas it is almost T-independent for T > 30 K hinting to SIS junctions [5]. This observation indicates the presence of intergrain weak-links of low quality containing flux. Their *flux-flow* losses saturate at $H_{rf} \sim 0.3$ mT at R_s(8.5GHz,0.3mT) ≈ 1 mΩ, superseded followed by a linear $R_s(H_{rf})$-increase for $H_{rf} \geq 0.3$ mT with $r \approx 0.5$. The latter fits to *hysteresis* Bean model type losses of Josephson fluxons entering and leaving Tl-2212 film in one half cycle [2]. In this case the surface resistance is described by

$$R_{hys}(H_{rf}, \omega) \cong (4\pi/3)\omega\mu_0(H_{rf}/2 j_{cJ}) \quad (3)$$

with j_{cJ} as the critical current density of Josephson fluxons. The temperature dependence of j_{cJ}(T) above $H^* \geq 0.3$ mT can be well described by $j_{cJ}(T/T_c) = j_{c0}(1\text{-}T/T_c)^m$, with m = 0.4, indicating dominant weak-link contribution to the critical current density. We note, that the critical current densities of j_{cJ}(77K) ≃ 2.4 MA/cm^2 obtained by $R_s(H_{rf})$-fits with Eq.(3), are comparable to the critical current densities obtained by inductive measurements at lower frequencies (see Table I). Comparatively, the j_{cJ}(77 K) ≃ 1 MA/cm^2 value obtained from $R_{res}(T)$ according to Eq.(2) is a factor of 2 smaller than the value given in Table I. These discrepancies are due to the fact that the detailed distribution of the weak-links is not taken into account.

It is remarkable, that because of the *non-linear* $R_s(H_{rf})$-behavior in the entire rf field range, $R_s(H_{rf} \rightarrow 0)$ losses can not be obtained for C007-3b. Extrapolating the $R_s(H_{rf})$-dependence to zero rf fields according to Eq.(1) yields negative values for *A* at $T \leq 40$ K like in [15].

Similar to C007-3b, above $H^* \geq 1$ mT C138-2a(A) shows a linear $R_s(H_{rf}) \propto H_{rf}$ dependence with slightly temperature dependent slopes in Fig.2 in line with Eq.(3) and a small flux-flow component of $\eta \leq 0.1$ mΩ (Table II). The linear increase together with the temperature independent $r \approx 1$ in Fig.4 and Table II, hint again to *hysteresis* losses by Josephson fluxons, like the $\delta R_s \propto \omega H_{rf}$ and $r \approx 1$ found for defective YBCO films [8]. Both, $\delta R_s \propto \omega H_{rf}$ with $r \approx 1$ or $\eta > 0$, can only be explained by an rf field component perpendicular to the thin film surface. This rf field component can be related to frozen-in flux [16], which is able to explain $\eta > 0$ with H_0 as flux-loss scaling field, and/or to morphological defects as, e.g., film thinning at the edge of the mode. The close relation of $\delta R_s \propto H_{rf}$ and $\eta > 0$ hint to weak links containing fluxons causing *flux-flow* losses saturating at $\mu_0 H_{rf} \sim 0.3$ mT. At $\mu_0 H_{rf} > 0.3$ mT (1 mT) for C007-3b (C138-2a) flux is able to penetrate into the film with a rate *f*/2 causing *hysteresis* losses.

The presence of holes yields edge enhanced fields with $R_s(H_{rf}) \propto H_{rf}^2$ dependencies in TE_{011}-modes (Fig.3). According to the calculations in [13] the *hysteresis* losses for the Bean critical state model lead to a $R_{slit} \propto \omega\mu_0\pi^3(gH_{rf})^2$ dependence, where the knowledge of hole dimension *g* and density are required for the quantification of losses in Fig.3. The nature of the hole field enhancement by bulging to the film back side is similar to the field-edge enhancement in the strip-line modes [17] leading to the flux penetration near the edges of the strip and explain the factor of 10 larger *C*-factors in Tl-2212 as compared to YBCO for similar R_s(77 K)-values [8]. The frequency dependence of parameter *C* (Table II and Fig.3) follows $C \propto \omega^\alpha$ with $\alpha \sim 0.3$ to 2 in line with *hysteresis losses* where $\alpha \sim 1$ is expected. The inset of Fig.3 shows the temperature dependence of turn-up field $H^*(T) \propto j_{cJ}(T)$, which can be well described by $H^*(T) = H^*(0\text{K})(1\text{-}(T/T_c)^2)$ proving Josephson fluxons to be responsible for the non-linearities in good agreement with the results on structured YBCO films [17]. The *r(T)*-values ≤ 10 being slightly temperature dependent (Table II) hint to *hysteresis* losses by Josephson fluxons. The *r*-values turn lower with higher R_s-values (higher temperatures), i.e., larger penetration depths enforce bulging at both 8.5 and 15.3 GHz, see Table II.

In summary, whereas good power handling is achieved in *high* quality Tl-2212 films with H^*(77K) ≥ 3 mT, *low* and *mid* quality films with H^*(77K) ~ 0.1 to 1 mT show new features. We quantified three different loss mechanisms in *mid* quality Tl-2212 films. Films of very low quality contain defects in form of very weak-links yielding *flux-flow* losses with $r \sim 0.5$ already at $H^* \leq 0.3$ mT. At higher rf field levels *hysteresis* losses appear originating in the nucleation and pinning of Josephson fluxons with a rate of *f*/2 leading to losses with a quadratic field dependence via field-enhancements at holes or cracks. The *C*-values are typically a factor 10 larger than for YBCO films [8], which may be related to larger j_c-values and less holes and cracks in a latter case. The origin and material science of the defects leading to enhanced nonlinearities in Tl-2212 films are under study.

ACKNOWLEDGMENT

We thank A. Meier for performing the R_s-mapping and P. Severloh for optical microscopy analysis. Useful discussions and suggestions of A. Gurevich are highly appreciated.

REFERENCES

[1] R. B. Hammond et al., *Microwave Journal* **41**, (1998); R. Arnott et al., "Advanced Base Station Technology", *IEEE Communications Magazine*, February (1998).
[2] J. Halbritter, *J. Superconductivity* **8**, (1995) 691; J. Halbritter, *Supercond. Sci. Technol*. **12**, (1999) 883.
[3] J. Halbritter, *J. Superconductivity* **14**, (2001) 9.
[4] M. Tinkham, "Introduction to superconductivity", *McGraw-Hill International Edition*, (1996).
[5] A. Gurevich et al., *Phys. Rev. Lett*. **88**, (2002) 097001.
[6] T.L. Hylton, Dissertation University of Stanford, California, (1991); T.L. Hylton et al., *Appl. Phys. Lett.* **53**, (1988) 1343.
[7] H. Xin et al., *Phys. Rev. B* **61**, (2000) R14952.
[8] E. Gaganidze et al., *IEEE Trans. Appl. Supercond.* **11**, (2001) 2808.
[9] E. Gaganidze et al., *Physica C*, accepted for publication.
[10] H.Schneidewind et al., *Supercond. Sci. Technol.* **14**, (2001) 200.
[11] J. Halbritter et al., *IEEE Trans. Appl. Supercond.* **11**, (2001) 3541.
[12] J. Halbritter et al., submitted to *Journal of Appl. Physics*.
[13] B.A. Willemsen et al., *Phys. Rev. B* **58**, (1998) 6650.
[14] J.R. Waldram, « Superconductivity of Metals and Cuprates », ISBN 085274 335 1hbK, *Institute of Physics Publishing, Techno House, Redeliffe Way*, Bristol BSI GNX UK, page 273.
[15] Y. M. Habib et al., *Phys. Rev. B* **57**, (1998) 13833.
[16] A.N. Grigorenko et al., *Appl. Phys. Lett.* **78**, (2001) 1586.
[17] Nguyen et al., *Phys Rev. B* **51**, 6686 (1995).